Zero- and Low-Speed Angle Observer for Bearingless Permanent Magnet Machines

T. Wellerdieck,
T. Nussbaumer,
J. W. Kolar

Zero- and Low-Speed Angle Observer for Bearingless Permanent Magnet Machines

Tobias Wellerdieck[1], Thomas Nussbaumer[2], and Johann W. Kolar[1],
[1]Power Electronic Systems Laboratory, ETH Zurich, Switzerland
[2]Levitronix GmbH, Zurich, Switzerland

Bearingless machines are successfully used for a variety of applications that demand for low mechanical losses, low wear and low contamination. These machines require exact knowledge of the radial and angular rotor position in order to ensure stable levitation. This information is obtained with different position sensors. Alternatively, a sensorless approach can be used to determine the rotor position. The omission of the angular sensors leads to a reduction in costs and an improvement in reliability and allows to explore new areas of applications for bearingless machines. However, few zero and low speed sensorless angle estimators are published to this date. Therefore, a novel estimator to determine the rotor angle at zero and at low speeds and thus allowing sensorless operation over the whole speed range of the bearingless permanent magnet synchronous machine is proposed in this paper. The observer utilizes the radial position measurements and a model of the bearing force generation to determine the error of the angular position estimation.

Index Terms—**Bearingless, Sensorless, Control, Observer.**

I. INTRODUCTION

A bearingless machine is an electric motor with an integrated magnetic bearing. The rotor of such a machine is levitated using a magnetic field. This eliminates the need for mechanical bearings and allows the rotor to be operated in a sealed compartment. Bearingless machines are well suited for applications with demands on high speeds, low wear and low particle generation and contamination [1]–[3].

This paper focuses on a bearingless permanent magnet disc drive [4], of which a schematic drawing is shown in Fig. 1. The rotor consists of a ring-shaped permanent magnet with a diameter that exceeds its axial length. This topology is chosen because it features passive stability in three degrees of freedom. Therefore, only three degrees of freedom have to be controlled actively [5], [6]. The control system utilizes information from displacement and angular sensors to achieve stable levitation and a high drive performance. The cost and complexity of the system can be reduced if an angle-sensorless control is used. This allows for new areas of operation for bearingless machines.

A similar development can be reported for electric machines with conventional bearings. Different ways of sensorless estimation of the rotor angle for permanent magnet machines are reported in the literature [7]–[10]. These methods can be divided into two categories: either the machine voltages and currents are measured to obtain information about the induced voltage and the rotor flux angle or high frequency signals are injected into the machine terminals to measure the phase inductances. The first approach requires a minimal amplitude of the induced voltage and thus can only be employed for medium and high speeds. The second approach works for all speed ranges. However, any rotor displacement in a bearingless machine will disturb the inductance measurement and, therefore, have a direct impact on the angle estimation. A

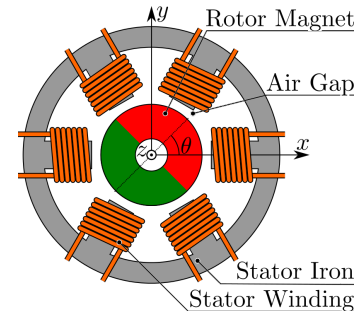Corresponding author: T. Wellerdieck (email: wellerdieck@lem.ee.ethz.ch).

Fig. 1: Schematic representation of the bearingless permanent magnet machine.

third approach is available for bearingless machines in which the radial displacement of the rotor can be used to obtain information about the rotor angle.

This paper proposes the usage of a novel zero- and lowspeed-angle observer to obtain the rotor angle based on observations of the radial bearing behaviour. The force and torque generation in a bearingless machine are described based on the flux density harmonics in the airgap. Subsequently, the influence of a rotor angle estimation error on the behaviour of the radial position control is examined. This serves as a basis for the formulation of the angle observer structure. The operational principle of the observer is investigated through simulations. Finally, the implementation of the method is discussed.

II. FORCE AND TORQUE CALCULATION

The radial forces and the torque acting upon the rotor of a bearingless machine can be calculated by using the Maxwell stress tensor [11]. The force and torque calculation neglects z components of the flux due to the axial symmetry of the bearingless disc drive. Therefore, it is sufficient to consider the radial and tangential flux components in the airgap. The

TABLE I: Relevant variables definingthe magnetic flux density in the airgap of a bearingless machine.

Description	Var.	Range
Displ. in x Direction	Δx	$\Delta x \in [-2\text{ mm}, 2\text{ mm}]$
Displ. in y Direction	Δy	$\Delta y \in [-2\text{ mm}, 2\text{ mm}]$
Rotor Angle	θ	$\theta \in [0, 2\pi]$
Drive Current	$\hat{I}_\mathrm{D}, \phi_\mathrm{D}$	$\hat{I}_\mathrm{D} \in [0, 5\text{ A}], \phi_\mathrm{D} \in [0, 2\pi]$
Bearing Current	$\hat{I}_\mathrm{B}, \phi_\mathrm{B}$	$\hat{I}_\mathrm{B} \in [0, 5\text{ A}], \phi_\mathrm{B} \in [0, 2\pi]$

TABLE II: Relevant field harmonics of the radial and tangential flux density components in the airgap ($k \in [r, t]$).

Description	Amplitude	Relevant Harmonics
Zero Displacement	$\hat{B}_{\mathrm{k,i},0} = \text{const}$	$i \in [1, 3, 5, 7]$
Rotor Displacmenet	$\hat{B}_{\mathrm{k,i},\Delta} \propto \sqrt{\Delta x^2 + \Delta y^2}$	$i \in [2, 4, 6, 8]$
Bearing Field	$\hat{B}_{\mathrm{k,i,B}} \propto \hat{I}_\mathrm{B}$	$i \in [2, 4, 8]$
Drive Field	$\hat{B}_{\mathrm{k,i,D}} \propto \hat{I}_\mathrm{D}$	$i \in [1, 5, 7]$

Fig. 2: Passive and bearing forces for a displaced rotor with zero angle estiamtion error (a) and non-zero angle estimation error (b).

calculation is carried out by integrating along the contour ξ shown in Fig. 2. The coordinate α depicts the position on ξ. Force and torque are calculated as

$$F_\mathrm{x} \propto \int_0^{2\pi} \left(B_\mathrm{r}^2 - B_\mathrm{t}^2\right) \cos\left(\alpha\right) - \left(2 B_\mathrm{t} B_\mathrm{r}\right) \sin\left(\alpha\right) d\alpha$$

$$F_\mathrm{y} \propto \int_0^{2\pi} \left(B_\mathrm{r}^2 - B_\mathrm{t}^2\right) \sin\left(\alpha\right) + \left(2 B_\mathrm{t} B_\mathrm{r}\right) \cos\left(\alpha\right) d\alpha \quad (1)$$

$$T_\mathrm{z} \propto \int_0^{2\pi} B_\mathrm{t} B_\mathrm{r} d\alpha.$$

The flux density components B_r and B_t can be approximated by their space harmonics $B_\mathrm{k,i}$ as

$$B_\mathrm{k}\left(\alpha\right) \approx \sum_i \hat{B}_\mathrm{k,i} \sin\left(i\alpha + \phi_\mathrm{k,i}\right), \ k \in [r, t]. \quad (2)$$

The amplitude $\hat{B}_\mathrm{k,i}$ and phase $\phi_\mathrm{k,i}$ of the space harmonics are dependent on the rotor position as well as the drive and bearing currents in the stator windings.

If magnetic saturation is neglected then the ith space harmonic of the magnetic flux density can be stated as

$$B_\mathrm{k,i} = B_{\mathrm{k,i},0}\left(\theta\right) + B_{\mathrm{k,i},\Delta}\left(\theta, \Delta x, \Delta y\right)$$
$$+ B_\mathrm{k,i,B}\left(\hat{I}_\mathrm{B}, \phi_\mathrm{B}\right) + B_\mathrm{k,i,D}\left(\hat{I}_\mathrm{D}, \phi_\mathrm{D}\right), \quad (3)$$

with the relevant variables listed in Tab. I. Table II lists the correlations between the parameters and the harmonics with $\hat{I}$ beeing the amplitude and ϕ beeing the phase of a current.

III. BEARING BEHAVIOUR

The radial position controller of a bearingless machine controls the bearing currents in the stator windings to ensure a stable levitation of the rotor at a given reference position x^*, y^*. The controller requires information about the radial position and the angle of the rotor magnet to achieve this task. It is assumed that the radial position is known exactly but the rotor angle is only estimated. The actual rotor angle is denoted by θ, the estimation by $\hat{\theta}$ and the error by $\Delta\theta = \hat{\theta} - \theta$.

Assume that $\theta = 0$, meaning that the rotor flux $\vec{\Psi}_\mathrm{R}$ is placed on the x axis, there is no angle estimation error, $\hat{\theta} = \theta$, and the rotor is at a reference rotor position $x^* > 0, y = 0$ as shown
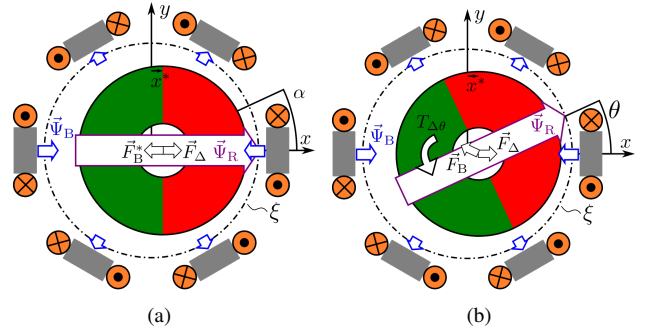
in Fig. 2(a). If higher flux density harmonics are neglected, the flux density components on the contour ξ are

$$B_\mathrm{r,1} = \hat{B}_\mathrm{r,1,0} \cos\left(\alpha\right)$$
$$B_\mathrm{t,1} = \hat{B}_\mathrm{r,1,0} \cos\left(\alpha - \pi/2\right)$$
$$B_\mathrm{r,2} = \hat{B}_\mathrm{r,2,\Delta} \cos\left(2\alpha\right) \quad (4)$$
$$B_\mathrm{t,2} = \hat{B}_\mathrm{t,2,\Delta} \cos\left(2\alpha - \pi/2\right)$$

with $\hat{B}_\mathrm{r,2} > \hat{B}_\mathrm{t,2}$. Inserting (4) into (1) shows that the radial displacement results in a force $\vec{F}_\Delta$. The bearing controller needs to generate a bearing force $\vec{F}_\mathrm{B}^*$ that compensates $\vec{F}_\Delta$. Therefore, the radial position controller imposes bearing currents in the stator coils leading to the bearing flux density harmonics

$$B_\mathrm{r,2,B} = \hat{B}_\mathrm{r,2,B} \cos\left(2\alpha + \pi\right)$$
$$B_\mathrm{t,2,B} = \hat{B}_\mathrm{t,2,\Delta} \cos\left(2\alpha + \pi/2\right), \quad (5)$$

which, accoring to (1), leads to a zero net force and zero torque.

However, if the rotor angle estimate is not correct then the bearing will behave differently. Assuming, that the rotor angle is changed to $\theta > 0$ as shown in Fig. 2(b). The passive flux density harmonics of order one and two are

$$B_\mathrm{r,1,0} = \hat{B}_\mathrm{r,1} \cos\left(\alpha - \theta\right)$$
$$B_\mathrm{t,1,0} = \hat{B}_\mathrm{r,1} \cos\left(\alpha - \theta - \pi/2\right)$$
$$B_\mathrm{r,2} = \hat{B}_\mathrm{r,2,\Delta} \cos\left(2\alpha - \theta\right) \quad (6)$$
$$B_\mathrm{t,2} = \hat{B}_\mathrm{t,2,\Delta} \cos\left(2\alpha - \theta - \pi/2\right).$$

Assume that the radial position controller has no information about the new rotor angle, meaning that the estimated angle $\hat{\theta} = 0 \Leftrightarrow \Delta\theta > 0$. Therefore, the bearing flux components are as given in (5). Inserting (5) and (6) into (1) results in

$$F_\mathrm{B,x} < F_\mathrm{B,x}^*, \ F_\mathrm{B,y} > F_\mathrm{B,y}^* = 0, \ T_\mathrm{z} < 0. \quad (7)$$

This shows that a rotor angle estimation error $|\Delta|\theta > 0$ has two effects on the bearing behaviour. First, the second order flux harmonics of a displaced rotor and the bearing

harmonics lead to a torque $T_{\Delta,z}$. The magnitude of this torque is proportional to the displacement. The torque is forcing the rotor angle to the estimated angle, driving the estimation error $\hat{\theta}$ to zero. Second, the angle estimation error leads to a deviation of the bearing force. The applied bearing forces $\vec{F}_B$ can be stated depending on the ideal bearing forces $\vec{F}_B^*$ and the rotor angle estimation error as

$$\vec{F}_B = \begin{bmatrix} \cos\left(\Delta\theta\right) & -\sin\left(\Delta\theta\right) \\ -\sin\left(\Delta\theta\right) & \cos\left(\Delta\theta\right) \end{bmatrix} \cdot \vec{F}_B^*. \qquad (8)$$

IV. OBSERVER STRUCTURE

The angle observer is based on the force coupling described in (8). The observer estimates the angle error $\Delta\hat{\theta}$ by evaluating the difference between the ideal bearing force $\vec{F}_B^*$ and the actual bearing force $\vec{F}_B$.

A simplified block diagram of the radial bearing with observer is shown in Fig 3. The two position controllers are labeled $C_x(s)$ and $C_y(s)$, the radial bearing is labeled $B(s)$ and the observer is labeled $O(s)$. The position controllers calculate the reference bearing currents I_{Bx}, I_{By} based on the deviation of the rotor position x, y from the reference position x^*, y^*. Block T denotes a park transformation, transforming the bearing currents to the stator frame. The transformed currents will lead to the forces F_x, F_y, which define the rotor movement together with any external forces $F_{x,e}, F_{y,e}$.
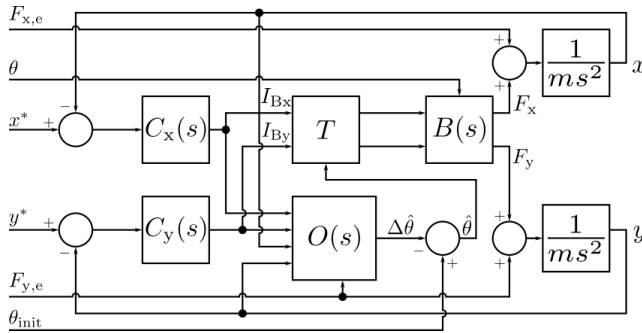

Fig. 3: Simplified block diagram of the radial bearing and the angle observer.

The functionality of the observer is shown in an example. First, the observer is used to estimate $\Delta\hat{\theta}$ but the observer loop is not closed, meaning that $\hat{\theta}$ is not changed.

Assume that a constant radial force $\vec{F}_{r,e}$ is pulling the rotor in the negative y direction. The rotor reference position and the initial rotor position and angle are randomly set to

$$x^* = y^* = 0, \;\; \theta_{init} = 60° \qquad (9)$$
$$x_{init} = y_{init} = -2 \text{ mm}.$$

Note that, $\Delta\hat{\theta}$ is not used to update $\hat{\theta}$, meaning that $\hat{\theta} = \theta_{init}$. Figure 4(a) shows the radial rotor position and that the rotor approaches the reference levitation position after 1 s. After 2 s the rotor is rotated by $15°$ by an external torque as shown in Fig. 4(b), which increases $\Delta\theta$. Figure 4(c) shows that the bearing currents during $1\text{ s} < t \leq 2\text{ s}$ are $I_{B,x} \approx 0$ mA, $I_{B,y} \approx 870$ mA. The currents are required to compensate $\vec{F}_{r,e}$. The angle of the ideal bearing force is

$$\angle\vec{F}_B^* = \arctan\left(\frac{I_{B,y}}{I_{B,x}}\right) = 90°. \qquad (10)$$

The bearing currents change to $I_{B,x} \approx -0.3$ mA, $I_{B,y} \approx 1$ A as θ is increased. The angle of the ideal bearing force becomes $\angle\vec{F}_B^* \approx 74°$ due to the radial bearing controllers that enforce $x \approx x^*, y \approx y^*$. The estimated error

$$\Delta\hat{\theta} = \arctan\left(\vec{I}_B\right) - \arctan\left(\vec{F}_{r,e}\right) - 180° \qquad (11)$$

is shown in Fig. 4(d). The observer estimates that the real rotor angle deviates from the estimated value by $\Delta\hat{\theta} \approx -16°$.
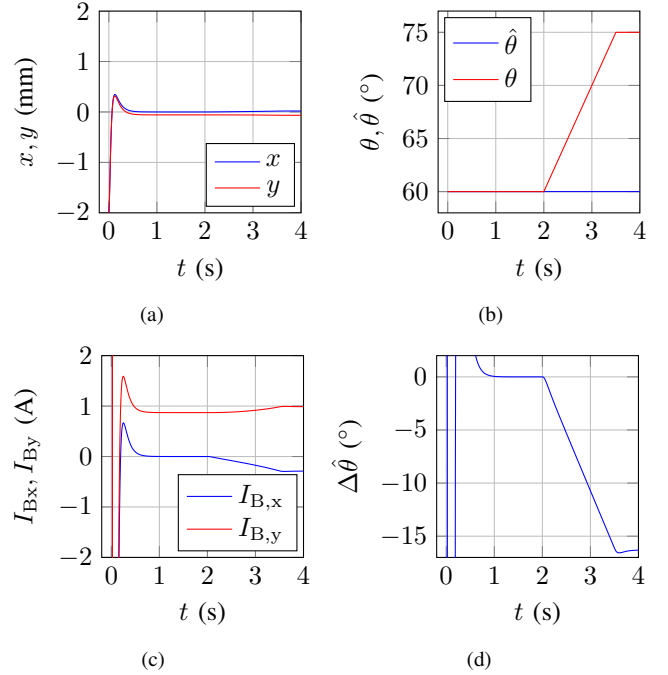

Fig. 4: Simulation of radial bearing performance with external force $\vec{F}_{r,e}$, radial rotor position (a), bearing currents (c), rotor angle and observer angle (b) and estimated angle error (d).

The observer loop is closed for the second example. This means that $\Delta\hat{\theta}$ is used to update $\hat{\theta}$. Also, the constant radial force is generated internally by setting the radial reference position such that

$$r^* = \sqrt{(x^*)^2 + (y^*)^2} > 0. \qquad (12)$$

This results in magnetic flux density harmonics as described in Tab. II and subsequently in a radial displacement force $\vec{F}_\Delta$ according to (1) that must be overcome by the bearing. This displacement force is used as $\vec{F}_{r,e}$ in equation (11) to determine the rotor angle.

Figure 5 shows the results of the simulation of the machine with full dynamics including higher order flux densities as listed in Tab. II. The reference rotor position is set to $x^* = 1$ mm, $y^* = 0$ mm, c.f. Fig. 5(a).

The estimated angle error $\Delta\hat{\theta}$ is calculated according to (11) and is used to update $\hat{\theta}$. Figure 5(b) shows the real rotor angle θ, which is unknown to the observer, and the estimate $\hat{\theta}$. The estimation error, shown in Fig. 5(c), is always less than $10°$. The rotor speed estimate is calculated by derivation of the angle estimate and is used for the drive current controller. Figure 5(d) shows the machine speed n, the reference speed n^* and the machine speed estimate $\hat{n}$. The machine speed is

constant after approximately 11 s. An integrator part is added to the observer

$$\hat{\theta}(t) = \theta_{\text{init}} + P_{\text{obs}} \cdot \Delta\hat{\theta}(t) + I_{\text{i}} \cdot \int_0^t \Delta\hat{\theta}(\tau)\, d\tau \qquad (13)$$

which drives the estimation error $\Delta\theta$ to zero once the rotor speed reaches the reference speed, c.f. Fig. 5(c). The integrator limits the usage of an integrator part in the speed controller since the interaction of the integrator in the observer and the integrator in the speed controller will lead to oscillations. The system can thus be optimized for either fast decay of the angle error or a small steady state speed error.
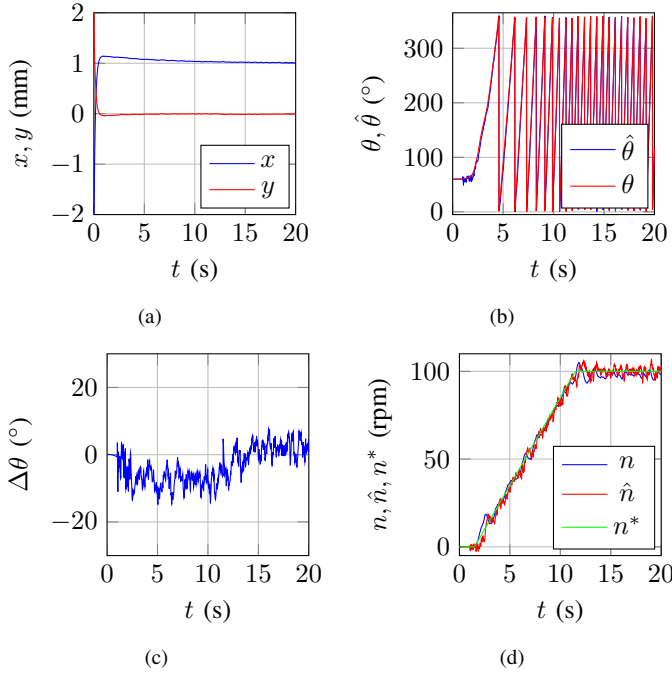

Fig. 5: Simulation of closed loop observer performance for acceleration from 0 to 100 rpm with radial rotor position (a), rotor angle and angle estimate (b), estimation error (c) and rotor speed and rotor speed estimate (d).

V. IMPLEMENTATION

Some requirements must be met when implementing the method for a bearingless machine. The initial rotor angle can be detected by the control scheme presented in [12]. The rotor can then be brought to levitation with this initial angle. The passive stability of the rotor angle estimate ascertains that the machine control is functional at zero speed. The radial position control will then evaluate the bearing currents during levitation to detect an external radial force. If such a force is available then the observer can utilize it to detect the rotor angle. Alternatively, the rotor reference position is set according to (12) to generate a sufficient displacement force. The rotor is then allowed to rotate freely and the drive control is used to accelerate the machine efficiently.

The observer method is based on the assumption that the radial forces acting upon the rotor are known. Any unknown disturbance force will lead to an angle estimation error $\Delta\hat{\theta}_\delta$ as shown in Fig. 6. The maximum acceptable, undetectable angle
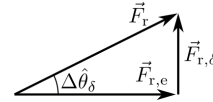

Fig. 6: Undetectable angle estimation error due to disturbance force.

estimation error $\Delta\hat{\theta}_\delta$ can be calculated utilizing the magnitude of the known radial force $|\vec{F}_{\text{r,e}}|$ and the magnitude of the disturbance force $|\vec{F}_{\text{r},\delta}|$ as

$$\Delta\hat{\theta}_\delta = \arctan\left(\frac{|\vec{F}_\delta|}{|\vec{F}_{\text{r,e}}|}\right). \qquad (14)$$

VI. CONCLUSION

The angle observer structure proposed in this paper allows the estimation of the rotor angle for zero and low speeds. It is based on the assumptions that the initial rotor angle is known and external radial forces are constant or small and utilizes the behaviour of the radial bearing to calculate a rotor angle estimation. Two different simulation cases show the observer performance for different modes of operation.

VII. ACKNOWLEDGEMENT

REFERENCES

[1] A. O. Salazar, A. Chiba, and T. Fukao, "A review of developments in bearingless motors," *Proc. 7th Int. Symp. Magnetic Bearings*, pp. 335–340, May 2000.

[2] J. Amemiya, A. Chiba, D. Dorrell, and T. Fukao, "Basic characteristics of a consequent-pole-type bearingless motor," *Magnetics, IEEE Transactions on*, vol. 41, pp. 82–89, Jan 2005.

[3] T. Tezuka, N. Kurita, and T. Ishikawa, "Design and simulation of a five degrees of freedom active control magnetic levitated motor," *Magnetics, IEEE Transactions on*, vol. 49, pp. 2257–2262, May 2013.

[4] X. Sun, L. Chen, and Z.Yang, "Overview of bearingless permanent-magnet synchronous motors," *Industrial Electronics, IEEE Transactions on*, vol. 60, no. 12, pp. 5528–5538, 2013.

[5] W. Gruber, S. Silber, W. Amrhein, and T. Nussbaumer, "Design variants of the bearingless segment motor," in *Power Electronics Electrical Drives Automation and Motion (SPEEDAM), 2010 International Symposium on*, pp. 1448–1453, June 2010.

[6] T. Nussbaumer, P. Karutz, F. Zurcher, and J. Kolar, "Magnetically levitated slice motors - an overview," *Industry Applications, IEEE Transactions on*, vol. 47, pp. 754–766, March 2011.

[7] J.-S. Kim and S.-K. Sul, "New approach for high-performance pmsm drives without rotational position sensors," *Power Electronics, IEEE Transactions on*, vol. 12, pp. 904–911, Sep 1997.

[8] H.-W. Park, S.-H. Lee, T.-H. Won, M.-S. Kim, and C.-U. Kim, "Position sensorless speed control scheme for permanent magnet synchronous motor drives," in *Industrial Electronics, 2001. Proceedings. ISIE 2001. IEEE International Symposium on*, vol. 1, pp. 632–636 vol.1, 2001.

[9] P. Acarnley and J. Watson, "Review of position-sensorless operation of brushless permanent-magnet machines," *Industrial Electronics, IEEE Transactions on*, vol. 53, pp. 352–362, April 2006.

[10] S.-Y. Kim and I.-J. Ha, "A new observer design method for hf signal injection sensorless control of ipmsms," *Industrial Electronics, IEEE Transactions on*, vol. 55, pp. 2525–2529, June 2008.

[11] K. Meessen, J. Paulides, and E. Lomonova, "Force calculations in 3-d cylindrical structures using fourier analysis and the maxwell stress tensor," *Magnetics, IEEE Transactions on*, vol. 49, pp. 536–545, Jan 2013.

[12] K. Raggl, B. Warberger, T. Nussbaumer, S. Burger, and J. Kolar, "Robust angle-sensorless control of a pmsm bearingless pump," *Industrial Electronics, IEEE Transactions on*, vol. 56, pp. 2076–2085, June 2009.